

# Epitaxial growth and exchange biasing of PdMn/Fe bilayers grown by ion-beam sputtering

Ning Cheng, JaePyoung Ahn, and Kannan M. Krishnan<sup>a)</sup>

*Materials Sciences Division, Lawrence Berkeley National Laboratory, University of California, Berkeley, California 94720*

Epitaxial PdMn/Fe bilayer structures, in both  $a$ -axis PdMn(100)/Fe(001)/MgO(001) and  $c$ -axis PdMn(001)/Fe(001)/MgO(001) orientations, were grown by ion-beam sputtering. The  $a$ -axis samples were grown at low temperatures ( $T < 280$  °C) while the  $c$ -axis films were stabilized at a higher temperature range ( $T > 300$  °C). Vibrating sample magnetometry measurements show that the as-grown  $a$ -axis samples do not have a measurable exchange bias while  $c$ -axis samples have an exchange bias field  $H_e \sim 33$  Oe. However, annealing at 230 °C for 40 min results in a measurable exchange ( $H_e \sim 10$  Oe) for  $a$ -axis samples due to chemical ordering. The possible cause for the difference of  $H_e$  in  $a$ -axis and  $c$ -axis orientations is also discussed. In addition to the normal structure, inverted structures were obtained epitaxially. The exchange biasing for Fe(001)/PdMn(001)/MgO(001) is as big as 68 Oe. © 2001 American Institute of Physics.

[DOI: 10.1063/1.1360677]

Exchange biasing between antiferromagnetic (AFM) and ferromagnetic (FM) layers in thin film form has attracted considerable technological interest because of the pinning effects of a FM by an AFM in magnetoresistance sensor and spin-valve heads.<sup>1</sup> However, in spite of the extensive studies conducted on various kinds of exchange-bias systems, its microscopic origin has remained a subject of debate.<sup>2</sup> NiMn, PtMn, and PdPtMn<sup>3-5</sup> are good candidates for technological applications because of their excellent corrosion resistance and large bias field. One of the difficulties in studying the exchange mechanism in these systems is due to the difficulty in obtaining good quality epitaxial samples with well controlled AFM/FM interfaces. PdMn alloys, belonging to the important family of CuAu-I-type structures, were grown epitaxially on Fe films by MBE.<sup>6</sup> Moreover, by inspecting the spin structure of bulk PdMn, we found that in the (001), (100), and (010) surfaces, the spin configuration is different. (001) gives a compensated surface while (010), (100) show an uncompensated surface. It would be of fundamental interest to reproducibly engineer the growth of these films along different crystallographic orientations to obtain films with (001) or (100) [or (010)] in plane. This should shed light on the relationship between different interface spin structures and  $H_e$  in PdMn, i.e., the orientation dependence of the exchange biasing effect and ultimately a better understanding of the exchange biasing mechanism.

The samples were grown in an ion-beam sputtering system with a base pressure of  $\sim 5 \times 10^{-9}$  Torr. The composition of the alloy target was Pd<sub>44</sub>Mn<sub>56</sub>. The deposition rate was 0.4 Å/s for Fe and 0.5 Å/s for PdMn and the thickness was controlled by a crystal thickness monitor. The Au cap layer was deposited to prevent the sample from oxidation. During the growth, an in plane biasing field of 500 Oe was

used. In the normal stacking sequence with Fe as the seed layer, epitaxial PdMn/Fe bilayer structures in both  $a$ -axis PdMn(100)/Fe(001)/MgO(001) and  $c$ -axis PdMn(001)/Fe(001)/MgO(001) orientations were obtained. In addition to the normal structure, inverted structures without any seed layers, both in the  $c$ -axis Fe(001)/PdMn(001)/MgO(001) and  $a$ -axis Fe(001)/PdMn(100)/MgO(001) orientations were obtained epitaxially. The thickness for all the four structures were Fe (70 Å), PdMn(300 Å). Structural details were obtained by x-ray diffraction (XRD) and transmission electron microscopy (TEM). The magnetic properties were measured by vibrating sample magnetometry.

Table I lists the structures, processing conditions and exchange biasing of a series of samples before and after annealing. Epitaxial films in both the  $a$ -axis and the  $c$ -axis orientations were successfully grown. The definition of  $a$ -axis and  $c$ -axis samples is shown in Fig. 1 based on the structure of bulk PdMn.<sup>7</sup> The  $a$ -axis samples were grown in a low temperature range ( $T < 280$  °C), the  $c$ -axis samples were stabilized at a higher temperature range ( $T > 300$  °C). The orientation relationship was confirmed by XRD and TEM.

Figure 2(a) shows the  $\vartheta-2\vartheta$  XRD scan; besides the (002) peak of MgO and Fe, there is a strong peak at  $\sim 52^\circ$

TABLE I. Structures, processing conditions, and exchange biasing of a series of PdMn/Fe samples.

| Grow temp.<br>(°C) | Direction | $H_e$      |                     | Ordering<br>(after ann.) |
|--------------------|-----------|------------|---------------------|--------------------------|
|                    |           | (as-grown) | (optimum ann.) (Oe) |                          |
| 50                 | $a$       | 0          | 8                   | Yes                      |
| 200                | $a$       | 0          | 10                  | Yes                      |
| 260                | $a$       | 0          | 9                   | Yes                      |
| 370                | $c$       | 30         | 35                  | Yes                      |
| 420                | $c$       | 32         | 32                  | Yes                      |
| 50                 | Inv.- $a$ | 0          | ...                 | ...                      |
| 420                | Inv.- $c$ | 68         | 68                  | Yes                      |

<sup>a)</sup> Author to whom correspondence should be addressed; electronic mail: krishnan@lbl.gov

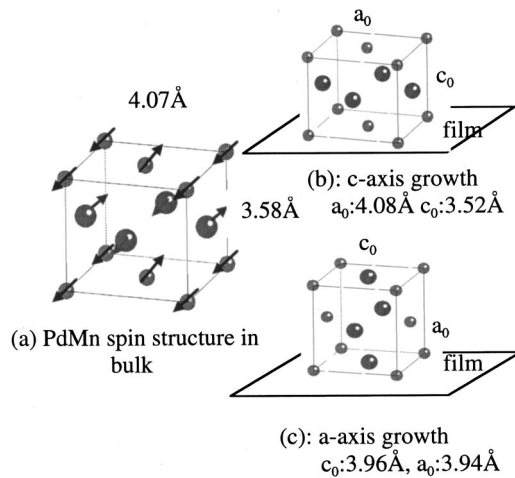


FIG. 1. (a) PdMn bulk spin structure and crystal structure (see Ref. 7). Crystal structure and unit cell parameters measured for *c*-axis oriented (b) and *a*-axis oriented films (c).

which corresponds to a lattice parameter of  $1.76 \text{ \AA}$ . This can be indexed as the PdMn (002) peak, which corresponds to a *c*-axis growth [see Fig. 1(b)]. Note that the PdMn (001) peak is also strong, indicating good chemical ordering in the as-grown *c*-axis sample. Figure 2(b) shows the XRD data for a low temperature growth sample. The peak at  $\sim 46^\circ$ , which corresponds to a lattice parameter of  $1.98 \text{ \AA}$ , can be indexed as the PdMn (200) peak and indicates *a*-axis growth [Fig. 1(c)]. In the latter case the chemically ordered (100) peak was not observed in XRD. This will be discussed later.

Table I also lists the measured values of  $H_e$  (exchange biasing field). The *c*-axis samples show  $H_e \sim 33 \text{ Oe}$  in the as-grown condition with no change upon annealing. For *a*-axis samples  $H_e \sim 0$  in the as-grown condition but show a measurable  $H_e \sim 10 \text{ Oe}$  after annealing at  $230^\circ \text{C}$  for 40 min.

The XRD symmetric  $\vartheta$ - $2\vartheta$  scan is only sensitive to the structure in a direction normal to the film surface, i.e., it is not sensitive to the structure or chemical order in the plane. Hence, complementary TEM selected area diffraction (SAD) measurements using plan-view samples were carried out. Figures 3(a) and 3(b) are the SAD patterns for the *a*-axis sample in the as-grown and annealed conditions, respectively. In the [100] zone-axis condition, additional 001 diffraction spots, absent in the as-grown sample [Fig. 3(a)], appear in samples annealed [Fig. 3(b)] at  $230^\circ \text{C}$ . These extra spots correspond to the chemical ordering of the Pd and Mn in the film plane. The TEM dark field images from the extra spots showing the ordered volume fraction indicate the *a*-axis and *c*-axis samples have a similar degree of ordering.<sup>8</sup> The absence of such chemical ordering for samples annealed at temperatures  $< 200^\circ \text{C}$  is clearly related to the lack of  $H_e$  in these samples. Table I shows that the magnetic properties and the chemical ordering are closely correlated. It is well known that PdMn is an ordered AFM,<sup>7</sup> i.e., if it is a chemically ordered CuAu-I structure, it is an antiferromagnet. But if it is chemically disordered, it is also magnetically disordered. Hence, for the disordered PdMn/Fe bilayers, no significant exchange biasing can be expected.

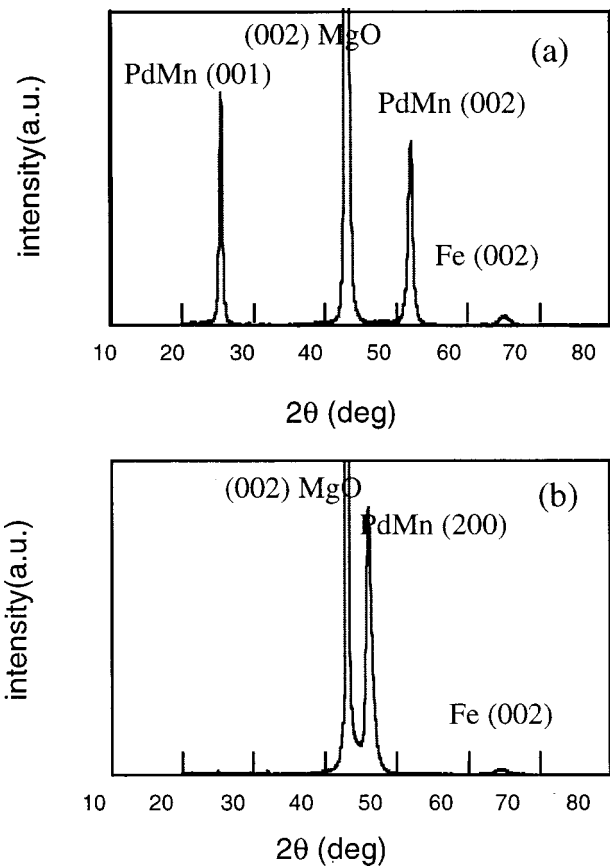


FIG. 2. X-ray diffraction scans for PdMn/Fe/MgO normal structure for *c*-axis oriented (a) and *a*-axis oriented (b) films.

The crystalline structures were studied by SAD using two zone axis orientations for *a*-axis ([100] [Figs. 3(a) and 3(b)], and [110] [Fig. 3(c)] zone axis). The SAD for *c*-axis samples, which show the similar fourfold in plane symmetry, is not shown here for brevity. In thin film form, the *c*-axis sample shows a structure similar to the bulk, i.e.,  $a_0 = 4.08 \text{ \AA}$ ,  $c_0 = 3.52 \text{ \AA}$  [Fig. 1(b)]. However, the *a*-axis sample is distorted with respect to the bulk with lattice parameters  $a_0 = 3.94 \text{ \AA}$ ,  $c_0 = 3.96 \text{ \AA}$  [Fig. 1(c)]; the distortion is likely due to the biaxial strain in the film to accommodate the epitaxial growth on the Fe/MgO. Both  $a_0$  and  $c_0$  measured by SAD are consistent with those values measured by XRD.

It is likely that the uniformly higher  $H_e$  observed for *c*-axis samples versus *a*-axis samples arises from the different spin structure at the PdMn/Fe interface because the other conditions, such as epitaxy, compositions, and degree of chemical ordering, are similar. A possible explanation assuming the bulk spin structure [Fig. 1(a)] may be as follows. For a *c*-axis orientated sample, the (001) interface plane is a spin compensated surface. For an *a*-axis oriented sample, the (001) interface plane [either (100), or (010)] is spin uncompensated. Hence the different spin structures at the interface may be the main cause for the difference in  $H_e$  for *a*-axis and *c*-axis samples. The result of the bigger  $H_e$  in *c*-axis samples which have the compensated surface agrees with the observation in other systems.<sup>9</sup> Further, the spin structure of the interface in such thin film structures may be different from the bulk because of changes in lattice parameter or symme-

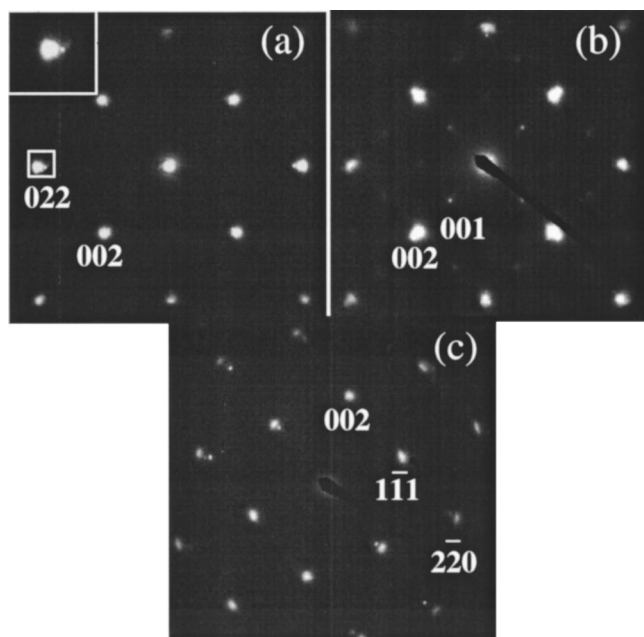


FIG. 3. TEM SAD patterns: (a)  $a$ -axis, as-grown, plan-view sample in the  $[100]$  zone axis shows only PdMn 002 and 022 diffraction spots. (b) 230 °C annealed  $a$ -axis oriented sample in the  $[100]$  zone axis shows both PdMn 002, 022, and PdMn 001 ordered diffraction spots. (c) SAD pattern from a tilted  $a$ -axis oriented as-grown plan-view sample in  $[110]$  zone axis. In all these figure the indexed spots are from PdMn films. The 022 (a) reflections are magnified in the insets and show splitting arising from the relaxation of the film. Single crystal MgO substrate reflections serve as an internal standard for lattice parameter calculation.

try. In this case, we can still safely conclude that the spin structures for the  $a$ -axis and  $c$ -axis oriented samples are different. In the case of  $c$ -axis growth, the interface will be occupied entirely by either Pd or Mn atoms. In the case of  $a$ -axis growth, it will always have nearly half Pd and half Mn atoms at the interface. Hence, the spin structure would be different at the interface. Other evidence for this interpretation is the strong correlation we observed between  $H_e$  and the relative intensities of the (002) and (200) XRD peaks in polycrystalline PdMn/Fe samples grown on Si substrates. A higher  $H_e$  is strongly correlated with a larger (002)/(200) intensity ratio. Hence it is likely that the uniformly higher  $H_e$  observed for  $c$ -axis samples versus  $a$ -axis samples arises from different spin structure at the interface. The ratio of  $a$ -axis crystals and  $c$ -axis crystals in polycrystalline films may be one of the important causes for the different  $H_e$  observed in polycrystalline samples of CuAu–I-type structure such as PtMn, MnNi, and PtPdMn, etc. Further study of the spin structure at interface using x-ray magnetic circular dichroism<sup>10</sup> is in progress.

We conclude with a brief discussion of the growth kinetics leading to the successful control of the crystallographic orientation of the PdMn films. With a lattice parameter of 4.07 Å, epitaxial growth of PdMn on Fe would minimize the lattice mismatch for the following orientation relationship: PdMn(001)||Fe(001) and PdMn[100]||Fe[110]; i.e., a  $c$ -axis

orientation is expected to grow preferentially to the  $a$  axis. However, if growth kinetics is also considered,  $a$ -axis growth is not difficult to imagine. The composition of the alloy sputtering target is Pd<sub>44</sub>Mn<sub>56</sub>. When it is sputtered, nearly the same amount of Pd and Mn reach the substrate simultaneously. If the substrate temperature is low, the atoms do not have enough energy to diffuse either between the layers or within the layer, the composition remains about Pd:Mn = 1:1 in each atomic layer. This is just a disordered  $a$ -axis sample. If it is grown at elevated temperatures, diffusion during growth occurs more readily than by solid state diffusion upon annealing. This helps the atoms to diffuse and reach the local minimum energy configuration, which in this case is the formation of a layer of roughly 100% Pd and then a layer of 100% Mn parallel to the growth plane, i.e., an ordered  $c$ -axis sample.

Finally, besides the normal structure, inverted structures (Table I) Fe(001)/PdMn(001)/MgO(001) and Fe(001)/PdMn(100)/MgO(001) were also grown epitaxially. With similar thickness of Fe and PdMn,  $H_e$  of 68 Oe was observed in Fe(001)/PdMn(001)/MgO(001) samples. This is the biggest exchange reported in this system.

In conclusion, the growth conditions for high quality epitaxial film in both  $c$ -axis and  $a$ -axis orientations have been established for PdMn/Fe. The ability to grow inverted structures makes this a good system to study the effect of interface spin structure on exchange in an intermetallic AFM system. The  $c$ -axis oriented as-grown samples are chemically well ordered and show  $H_e$  of 33 Oe. For  $a$ -axis orientation, as-grown samples are not chemically ordered and do not show any  $H_e$ . After optimum annealing, the  $a$ -axis samples also become chemically ordered and show  $H_e$  of 10 Oe. The uniformly higher  $H_e$  observed for  $c$ -axis samples (when compared with the  $a$ -axis annealed samples) may arise from the different spin structure at the interface. Finally the ratio of  $a$ -axis and  $c$ -axis crystals may explain the difference in  $H_e$  observed in polycrystalline samples of PtMn and NiMn.

This work was supported by the U.S. Department of Energy, under Contract No. DE-AC03-76SF00098. The authors would like to thank R. F. C. Farrow for helpful discussions and C. Echer for assistance in TEM measurements.

<sup>1</sup>C. Tsang, M. M. Chen, and T. Yogi, Proc. IEEE **81**, 1344 (1993).

<sup>2</sup>J. Nogues and I. K. Schuller, J. Magn. Magn. Mater. **192**, 203 (1999).

<sup>3</sup>T. Lin, G. L. Gorman, and C. Tsang, IEEE Trans. Magn. **32**, 3443 (1996).

<sup>4</sup>R. F. C. Farrow, R. F. Marks, S. Gider, A. C. Marley, S. S. P. Parkin, and Mauri, J. Appl. Phys. **81**, 4986 (1997).

<sup>5</sup>H. Kishi, Y. Kitade, Y. Miyake, A. Tanaka, and K. Kobayashi, IEEE Trans. Magn. **32**, 3380 (1996).

<sup>6</sup>Y. J. Tang, B. Roos, T. Mewes, B. Hillebrands, and Y. J. Wang, Appl. Phys. Lett. **75**, 707 (1999).

<sup>7</sup>H. P. J. Wijn, *Magnetic Properties of Metals* (Springer, New York 1991), p. 83.

<sup>8</sup>N. Cheng, Ph.D. thesis, University of California, Berkeley, 2001.

<sup>9</sup>J. Nogues, T. J. Moran, D. Lederman, and I. K. Schuller, Phys. Rev. B **59**, 6984 (1999).

<sup>10</sup>N. Cheng, K. M. Krishnan, E. Girt, R. F. C. Farrow, R. F. Marks, A. Kellock, A. Young, and C. Huan, J. Appl. Phys. **87**, 6647 (2000).